A Cortisol-Based Energy Decoder for Investigation of Fatigue in Hypercortisolism

Dilranjan S. Wickramasuriya, *Student Member, IEEE* and Rose T. Faghih, *Member, IEEE*

***Abstract*— Hormones play a fundamental role in homeostasis. We develop a state-space model relating the body's internal energy to cortisol hormone secretions. Cortisol is secreted in pulses and follows a 24 h circadian rhythm. Secretory event timings carry important information regarding internal feedback signaling taking place, as do the upper and lower serum cortisol levels. We relate an internal energy state variable to cortisol pulse timings and to the upper and lower serum cortisol envelopes. We derive Bayesian filter equations for state estimation and use the Expectation-Maximization algorithm for model parameter recovery. Results on multi-day simulated data show circadian energy variations in healthy subjects and non-circadian fluctuations throughout 24 h periods in patient models suffering from hypercortisolism. The results shed new light on why patients diagnosed with excess cortisol disorders frequently experience symptoms of daytime fatigue and sleep disturbances at night. The state-space model is also an important first step towards the design of closed-loop controllers for treating hormone-related disorders in a manner that closely emulates the body's own pulsatile feedback mechanisms.**

I. INTRODUCTION

Hormones play a critical role in regulating the body's internal environment. Cortisol, belonging to the category of glucocorticoids, is the body's primary stress hormone. Its main purpose is to raise blood glucose levels and give the body more energy in response to external stressors [1]. Most cortisol disorders involve either too much (*hyper*cortisolism) or too little (*hypo*cortisolism) of the hormone. Cortisol is secreted in pulses, and between 15–22 pulsatile secretions occur each day in a healthy adult [2]. Cortisol is directly related to how energized or drowsy a person feels. Sweat-based sensor patches enable the possibility of using wearable technologies for treating cortisol disorders [3].

State-space models governing cortisol secretion dynamics have been developed previously (e.g. [4]). However, none of them explicitly take into account the pulsatile secretory nature *and* relate cortisol to the underlying state the human body is actually attempting to maintain within a desirable range. Motivated by cortisol's fundamental role in giving the body more energy by raising blood glucose levels, we present a state-space model relating cortisol secretions to the body's internal energy state. We relate this energy state to the pulsatile secretory events, and to the upper and lower serum cortisol envelopes. We use a combination of Bayesian filtering and Expectation-Maximization (EM) for state estimation and model parameter recovery.

*DSW and RTF are with the Department of Electrical and Computer Engineering at the University of Houston, Houston, TX 77004 USA (e-mail:{dswickramasuriya, rtfaghih}@uh.edu). This work was supported in part by NSF grant 1755780 – CRII: CPS: Wearable-Machine Interface Architectures. Correspondence should be addressed to senior author RTF.

II. METHODS

In the absence of experimental data spanning multiple days, we simulate cortisol measurements using the statistical models described in [5] and [6] for healthy subjects and Cushing's disease patients respectively. Cushing's disease is a type of hypercortisolism that can be triggered by tumors or prolonged drug use [7].

A. Data Simulation – Healthy Subject

Following [5], we draw pulse inter-arrival times for cortisol from a Gamma distribution with parameters $\alpha = 54$ and $\beta = 39$. These parameters are for inter-arrivals in terms of hours and are converted to minutes during simulation. The pulse amplitudes H_k follow a time-of-day-dependent Gaussian distribution $H_k \sim \mathcal{N}(\mu_k, \kappa_k^2)$ where $\mu_k = 6.1 + 3.93\sin\left(\frac{2\pi k}{1440}\right) - 4.75\cos\left(\frac{2\pi k}{1440}\right) - 2.53\sin\left(\frac{4\pi k}{1440}\right) - 3.76\cos\left(\frac{4\pi k}{1440}\right)$, $\kappa_k = \lambda\sqrt{\mu_k}$ and $\lambda = 0.1$ [5]. Given a vector of pulse input timings and amplitudes, we follow the solution of the coupled differential equations regulating the secretion of cortisol outlined in [8], [9] to obtain the serum cortisol profile over five days. We also use cortisol infusion and clearance rates of 0.0751 min^{-1} and 0.0086 min^{-1} based on the median rate parameters in [2] extracted for ten healthy subjects. Noise with standard deviation 0.5 μgdL^{-1} is finally added to the simulated observations.

B. Data Simulation – Cushing's Disease

1) No Circadian Rhythm: Lee *et al.* [6] suggest inter-arrival times of 59 ± 11 min with amplitudes of 38 ± 2.5 $\mu\text{gdL}^{-1}\text{min}^{-1}$ for simulating the serum cortisol profile of a male Cushing's disease patient recruited in a study originally described in [10]. We use the Gamma and Gaussian distribution parameters corresponding to the Cushing's mean and standard deviation values above to simulate a second set of inter-arrival times and amplitudes respectively.

2) With Circadian Rhythm: Berg *et al.* [10] noted the preservation of a cortisol circadian rhythm in a few Cushing's disease patients. We therefore simulate data for another hypothetical patient—one whose circadian rhythm was preserved by means of the time-of-day-dependent Gaussian pulse amplitudes. We set $\lambda = 2.5/\sqrt{38}$ when calculating the new pulse-amplitude standard deviation. We select $\mu_k = 38.5 + 1.93\sin\left(\frac{2\pi k}{1440}\right) - 1.6\cos\left(\frac{2\pi k}{1440}\right) - 1.5\sin\left(\frac{4\pi k}{1440}\right) - 3.5\cos\left(\frac{4\pi k}{1440}\right)$ to produce amplitudes in the same approximate range as for the first Cushing's disease patient with the same Gamma inter-arrival distribution and simulate a third set of measurements.

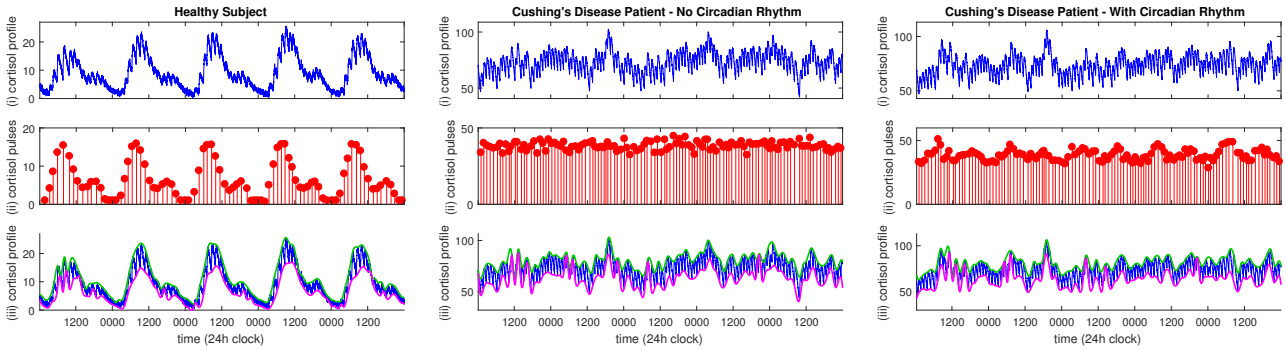

Fig. 1: **Cortisol profiles in a healthy subject and in Cushing's disease patients.** In each sub-figure, the sub-panels from top to bottom respectively depict, (i) the serum cortisol profile in μgdL^{-1}; (ii) the pulsatile secretions in $\mu gdL^{-1}min^{-1}$; (iii) the upper (green) and lower (mauve) envelopes of the cortisol profile. Note that serum cortisol measurements are much higher in Cushing's disease.

C. State-space Model

Prior work on estimating a latent state from point process and continuous-valued observations has frequently made use of first-order autoregressive and random walk models [11], [12], [13]. Here, we introduce a slight variation to explicitly account for circadian rhythmicity and assume that the body's internal energy state X_k evolves with time as follows:

$$X_k = \rho X_{k-1} + I_k + \varepsilon_k \tag{1}$$

$$I_k = \sum_{i=1}^{2} a_i \sin\left(\frac{2\pi ik}{1440}\right) + b_i \cos\left(\frac{2\pi ik}{1440}\right) \tag{2}$$

where $\varepsilon_k \sim \mathcal{N}(0, \sigma_\varepsilon^2)$; ρ is a coefficient to be determined along with the a_i and b_i terms. I_k acts as a forcing function in keeping with known energy variations during wakefulness and sleep in a 24 h period. It is generally taken that the circadian secretory pattern of adrenocorticotropic hormone (ACTH) imposes the same rhythm on cortisol [4].

We analyze our data at a time resolution of one minute (24 h = 1440 min). The presence or absence of a cortisol pulse each minute forms a binary point process and we assign $M_k = \{1, 0\}$ accordingly. The occurrence of a cortisol pulse at each time instant is therefore a Bernoulli distributed random variable with probability p_k. Following the theory of generalized linear models, we use a logit transformation [14] to relate p_k to the energy state X_k.

$$\log\left(\frac{p_k}{1-p_k}\right) = \beta_0 + \beta_1 X_k, \tag{3}$$

where β_0 and β_1 are coefficients to be determined. We also have the simulated daily serum cortisol measurements that the body is regulating based on energy demand and expenditure. We calculate their upper and lower envelopes using MATLAB's *envelope* function (Fig. 1). Here, we use the *peak* option to detect the envelopes as spline interpolations over local extrema. Labeling the upper and lower envelopes as R_k and S_k respectively, we assume linear relationships with X_k similar to [12].

$$R_k = \gamma_0 + \gamma_1 X_k + V_k \tag{4}$$

$$S_k = \delta_0 + \delta_1 X_k + W_k \tag{5}$$

where $V_k \sim \mathcal{N}(0, \sigma_V^2)$ and $W_k \sim \mathcal{N}(0, \sigma_W^2)$. $\gamma_0, \gamma_1, \delta_0, \delta_1$ are regression coefficients.

A modification to the upper and lower envelopes was necessary in the case of Cushing's disease where the levels of serum cortisol are much higher. This elevation is likely due to a malfunctioning of the feedback control mechanism governing the secretion of cortisol [7]. For a healthy subject, the serum cortisol levels can decrease to a value close to zero, although not to zero itself. Therefore, we can assume that zero forms a *lower baseline*. We hypothesize that the control system malfunction in Cushing's is caused by the body establishing a *new* lower baseline that cortisol levels are not allowed to drop below. This lower baseline is much higher than normal and is likely caused by the body gradually developing a resistance to the chronically high levels of cortisol. For both of the Cushing's patients we take the minimum cortisol level across the five days as the lower baseline and subtract it from the cortisol profile to obtain the modified upper and lower envelopes.

D. Estimation

1) Expectation-Step: Let $\mathcal{M}^k = \{M_1, M_2, \ldots, M_k\}$, $\mathcal{R}^k = \{R_1, R_2, \ldots, R_k\}$ and $\mathcal{S}^k = \{S_1, S_2, \ldots, S_k\}$ denote the observations up to time k. Taking $\mathcal{Y}^k = \{\mathcal{M}^k, \mathcal{R}^k, \mathcal{S}^k\}$ we wish to estimate $X_k \ \forall k$. The present work is a novel filter extending [12] with an additional continuous variable and a different state equation for estimating X_k. We therefore derive the following EM algorithm. We make a Gaussian approximation to the posterior density $f_{X_k|\mathcal{Y}^k}(x_k|y^k)$ similar to [13] and obtain the following set of Kalman-like forward filter equations for $k = 2 : K$.

Predict:

$$x_{k|k-1} = \rho x_{k-1|k-1} + I_k \tag{6}$$

$$\sigma^2_{k|k-1} = \rho^2 \sigma^2_{k-1|k-1} + \sigma_\varepsilon^2 \tag{7}$$

Update:

$$C_k = \frac{\sigma^2_{k|k-1}}{\sigma_V^2\sigma_W^2 + \sigma^2_{k|k-1}(\gamma_1^2\sigma_W^2 + \delta_1^2\sigma_V^2)} \tag{8}$$

$$\begin{aligned} x_{k|k} = x_{k|k-1} + C_k \Big[& \beta_1 \sigma_V^2 \sigma_W^2 (m_k - p_{k|k}) \\ & + \gamma_1 \sigma_W^2 (r_k - \gamma_0 - \gamma_1 x_{k|k-1}) \\ & + \delta_1 \sigma_V^2 (s_k - \delta_0 - \delta_1 x_{k|k-1}) \Big] \end{aligned} \tag{9}$$

$$\sigma^2_{k|k} = \left[\frac{1}{\sigma^2_{k|k-1}} + \beta_1^2 p_{k|k}(1-p_{k|k}) + \frac{\gamma_1^2}{\sigma_V^2} + \frac{\delta_1^2}{\sigma_W^2}\right]^{-1} \tag{10}$$

$p_{k|k} = \left[1 + e^{-(\beta_0+\beta_1 x_{k|k})}\right]^{-1}$ causes $x_{k|k}$ to appear on both sides of (11) and has to be solved numerically using Newton's method. The smoothed states $x_{k|K}$ and variances $\sigma^2_{k|K}$ are then obtained following the method given in [15].

2) Maximization-Step: The parameters $a_1, a_2, b_1, b_2, \rho, \beta_0, \beta_1, \gamma_0, \gamma_1, \delta_0, \delta_1, \sigma_V^2, \sigma_W^2, \sigma_\varepsilon^2$ are chosen at each M-step iteration to maximize the complete data log-likelihood. Defining the following terms

$$A_k \triangleq \rho \frac{\sigma^2_{k|k}}{\sigma^2_{k+1|k}} \tag{11}$$

$$U_k \triangleq x^2_{k|K} + \sigma^2_{k|K} \tag{12}$$

$$U_{k,k+1} \triangleq x_{k|K} x_{k+1|K} + A_k \sigma^2_{k+1|K}, \tag{13}$$

the parameter updates at the $(n+1)^{\text{th}}$ M-step iteration are

$$\rho^{(n+1)} = \frac{\sum_{k=1}^{K-1} U_{k,k+1}}{\sum_{k=1}^{K-1} U_k} \tag{14}$$

$$\begin{bmatrix} \gamma_0^{(n+1)} \\ \gamma_1^{(n+1)} \end{bmatrix} = \begin{bmatrix} K & \sum_{k=1}^{K} x_{k|K} \\ \sum_{k=1}^{K} x_{k|K} & \sum_{k=1}^{K} U_k \end{bmatrix}^{-1} \cdot \begin{bmatrix} \sum_{k=1}^{K} r_k \\ \sum_{k=1}^{K} r_k x_{k|K} \end{bmatrix} \tag{15}$$

$$\begin{aligned} \sigma_V^{2(n+1)} = \frac{1}{K}\Bigg[& \sum_{k=1}^{K} r_k^2 + K\gamma_0^{2(n+1)} + \gamma_1^{2(n+1)} \sum_{k=1}^{K} U_k \\ & - 2\gamma_0^{(n+1)} \sum_{k=1}^{K} r_k - 2\gamma_1^{(n+1)} \sum_{k=1}^{K} x_{k|K} r_k \\ & + 2\gamma_0^{(n+1)}\gamma_1^{(n+1)} \sum_{k=1}^{K} U_k \Bigg] \end{aligned} \tag{16}$$

$$\begin{aligned} \sigma_\varepsilon^{2(n+1)} = \frac{1}{K}\Bigg[& \sum_{k=2}^{K} U_k - 2\rho^{(n+1)} \sum_{k=1}^{K-1} U_{k,k+1} \\ & + \rho^{2(n+1)} \sum_{k=1}^{K-1} U_k - 2\sum_{k=2}^{K} I_k x_{k|K} \\ & + 2\rho^{(n+1)} \sum_{k=2}^{K} I_k x_{k-1|K} + \sum_{k=1}^{K} I_k^2 \Bigg]. \end{aligned} \tag{17}$$

The updates for $\delta_0, \delta_1, \sigma_W^2$ can be obtained likewise by replacing r_k with s_k in (15) and (16) respectively. Moreover, we have taken $X_0 = X_1$ rather than estimating it as a separate parameter as in one of the options provided in [11], [12]. This permits a certain amount of bias at the beginning. Solving for $\{a_i, b_i\}_{i=1,2}$ and ρ must be performed simultaneously. Here, we have separated them out to simplify computation. a_1, a_2, b_1, b_2 are chosen to minimize

$$Q_1 = \sum_{k=1}^{K} I_k^2 - 2\sum_{k=2}^{K} I_k x_{k|K} + \rho^{(n+1)} \sum_{k=2}^{K} I_k x_{k-1|K}. \tag{18}$$

Solving for $\{\beta_0, \beta_1\}$ requires calculating the partial derivatives of the following term.

$$Q_2 = \sum_{k=1}^{K} \mathbb{E}\Big[m_k(\beta_0 + \beta_1 X_k) - \log\left(1 + e^{\beta_0+\beta_1 X_k}\right)\Big] \tag{19}$$

We apply a Taylor series expansion around each $x_{k|K}$ similar to [13] and use MATLAB's *fsolve* to do so.

III. RESULTS

Fig. 1 shows the simulated cortisol profiles for the healthy subject and both Cushing's disease patients without and with

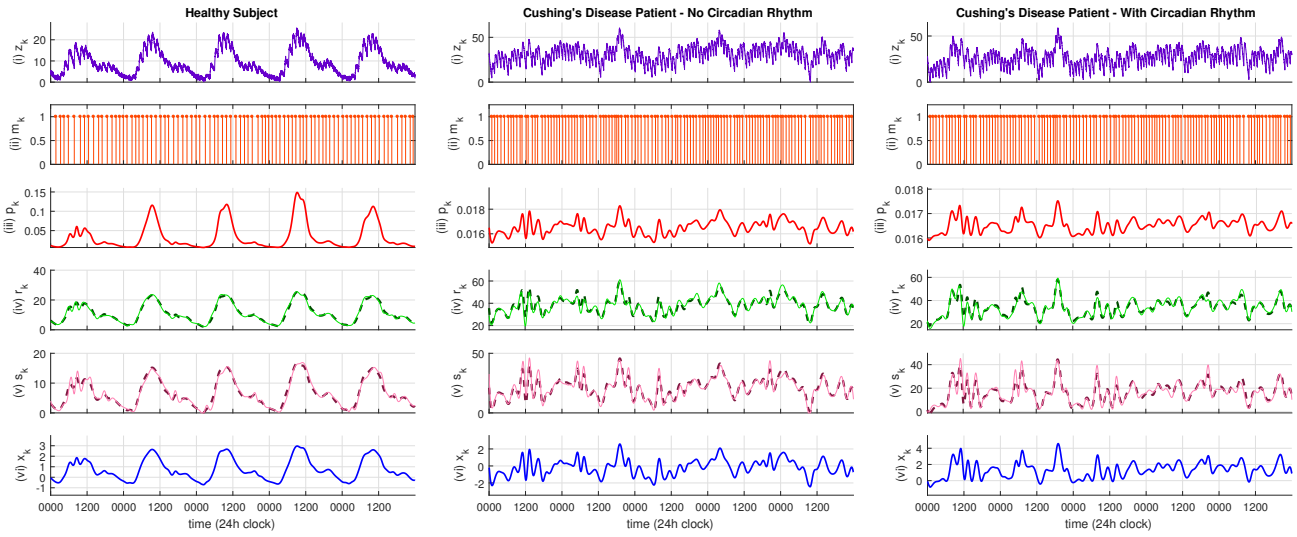

Fig. 2: **Cortisol-related energy state estimation.** In each sub-figure, the sub-panels in turn depict, (i) the cortisol level z_k; (ii) the pulse occurrences; (iii) the probability of pulse occurrence $p_{k|K}$; (iv) the true upper bound (green line) and its fit (dashed line); (v) the true lower bound (pink line) and its fit (dashed line); (vi) the energy estimate $x_{k|K}$. A clear circadian energy variation can be seen in the healthy subject while no such circadian rhythm is visible in the patients.

the circadian rhythm. To conform to the general range of serum cortisol levels, we use a starting value of 5 μgdL^{-1} for the healthy subject and 75 μgdL^{-1} for the patients.

Energy state estimates and fits to the observations are shown in Fig. 2. The healthy subject's energy state varies fairly consistently following circadian periodicity. The larger energy peak appears between 6:00–10:00 a.m. as expected, and a slight drop occurs in the afternoon. A secondary peak occurs between late afternoon and early evening.

No such circadian energy variation is seen for the first Cushing's disease patient. There are significant nighttime energy increases and daytime drops. This is expected as the simulations used a non-circadian probability distribution.

Interestingly, the second Cushing's disease patient also does not exhibit circadian energy variations despite the amplitudes being drawn from a Gaussian distribution with a circadian mean. We use coefficients for the sinusoids that do not give rise to a circadian rhythm with peaks as prominent as for the healthy subject. Moreover, the λ is also larger than 0.1. While the pulse amplitudes (Fig. 1) for this patient do follow a somewhat repetitive pattern, the serum cortisol levels do not exhibit that same pattern. It is likely that the Gamma distributed inter-arrival times for Cushing's cause this circadian rhythm disruption.

IV. DISCUSSION AND CONCLUSIONS

A healthy subject regularly experiences more energy during hours of wakefulness than during sleep. Recall that cortisol primarily raises blood glucose levels. One would expect therefore, that unusually high cortisol levels in a Cushing's disease patient constantly provides more energy. Instead, patients frequently experience fatigue and insomnia [16], [17]. While several factors could underlie this phenomena, we present a new perspective purely based on the energy state model. Our analysis offers the explanation that fatigue during the day and sleep disturbances at night could be due to the way in which energy varies during each 24 h period. For Cushing's patients, drops in energy are frequently seen in the daytime, as are increases during the night and likely cause daytime fatigue and nighttime sleeping difficulties.

We presented a state-space model relating energy to cortisol. We simulated data for a healthy subject and two Cushing's disease patients. The model offers new insight to the seemingly contradictory phenomena that fatigue and insomnia accompany excess blood cortisol. Due to the limited availability of blood cortisol measurements spanning multiple days, especially in pathological cases, our work had to rely on simulated data. Future work would involve further validation with simulated healthy subject data and validation on experimental data with larger samples in hypercortisolism. Incorporating ACTH secretions [18] and developing a closed-loop pulsatile controller [19] for treating cortisol-related disorders in a manner that mimics the body's own physiology are some other future directions. Moreover, modeling ε_k in (1) with a Cauchy distribution instead of a Gaussian would enable X_k to follow sharp temporal changes. The EM algorithm also has a tendency to converge to parameters where there is an overfit to one of the continuous-valued observations. This can be prevented with an early-stopping criteria similar to that used when training a neural network via gradient descent.

REFERENCES

[1] A. Esposito and V. Bianchi, *Cortisol: Physiology, Regulation and Health Implications*. Nova Science Publishers, 2012.

[2] R. T. Faghih, M. A. Dahleh, G. K. Adler, E. B. Klerman, and E. N. Brown, "Deconvolution of serum cortisol levels by using compressed sensing," *PloS One*, vol. 9, no. 1, p. e85204, 2014.

[3] M. Sekar, M. Pandiaraj, S. Bhansali, N. Ponpandian, and C. Viswanathan, "Carbon fiber based electrochemical sensor for sweat cortisol measurement," *Scientific Reports*, vol. 9, no. 1, p. 403, 2019.

[4] Z. Liu, A. R. Cappola, L. J. Crofford, and W. Guo, "Modeling bivariate longitudinal hormone profiles by hierarchical state space models," *J. American Statistical Association*, vol. 109, no. 505, pp. 108–118, 2014.

[5] E. N. Brown, P. M. Meehan, and A. P. Dempster, "A stochastic differential equation model of diurnal cortisol patterns," *American J. Physiology-Endocrinology and Metabolism*, vol. 280, no. 3, pp. E450–E461, 2001.

[6] M. A. Lee, N. Bakh, G. Bisker, E. N. Brown, and M. S. Strano, "A pharmacokinetic model of a tissue implantable cortisol sensor," *Advanced Healthcare Materials*, vol. 5, no. 23, pp. 3004–3015, 2016.

[7] H. Raff and T. Carroll, "Cushing's syndrome: from physiological principles to diagnosis and clinical care," *The J. of Physiology*, vol. 593, no. 3, pp. 493–506, 2015.

[8] R. T. Faghih, *System identification of cortisol secretion: Characterizing pulsatile dynamics*. PhD thesis, Massachusetts Institute of Technology, 2014.

[9] R. T. Faghih, "From physiological signals to pulsatile dynamics: A sparse system identification approach," in *Dynamic Neuroscience*, pp. 239–265, Springer, 2018.

[10] G. Van den Berg, M. Frölich, J. D. Veldhuis, and F. Roelfsema, "Combined amplification of the pulsatile and basal modes of adrenocorticotropin and cortisol secretion in patients with Cushing's disease: evidence for decreased responsiveness of the adrenal glands," *The J. Clinical Endocrinology & Metabolism*, vol. 80, no. 12, pp. 3750–3757, 1995.

[11] A. C. Smith, L. M. Frank, S. Wirth, M. Yanike, D. Hu, Y. Kubota, A. M. Graybiel, W. A. Suzuki, and E. N. Brown, "Dynamic analysis of learning in behavioral experiments," *J. Neuroscience*, vol. 24, no. 2, pp. 447–461, 2004.

[12] M. J. Prerau, A. C. Smith, U. T. Eden, Y. Kubota, M. Yanike, W. Suzuki, A. M. Graybiel, and E. N. Brown, "Characterizing learning by simultaneous analysis of continuous and binary measures of performance," *J. Neurophysiology*, vol. 102, no. 5, pp. 3060–3072, 2009.

[13] T. P. Coleman, M. Yanike, W. A. Suzuki, and E. N. Brown, "A mixed-filter algorithm for dynamically tracking learning from multiple behavioral and neurophysiological measures," *The Dynamic Brain: An Exploration of Neuronal Variability and its Functional Significance*, pp. 3–28, 2011.

[14] P. McCullagh and J. A. Nelder, *Generalized Linear Models*, vol. 37. CRC press, 1989.

[15] J. M. Mendel, *Lessons in Estimation Theory for Signal Processing, Communications and Control*. Pearson Education, 1995.

[16] V. D'Angelo, G. Beccuti, R. Berardelli, I. Karamouzis, C. Zichi, R. Giordano, M. A. Minetto, M. Maccario, E. Ghigo, and E. Arvat, "Cushings syndrome is associated with sleep alterations detected by wrist actigraphy," *Pituitary*, vol. 18, no. 6, pp. 893–897, 2015.

[17] L.-U. Wang, T.-Y. Wang, Y.-M. Bai, J.-W. Hsu, K.-L. Huang, T.-P. Su, C.-T. Li, W.-C. Lin, T.-J. Chen, and M.-H. Chen, "Risk of obstructive sleep apnea among patients with Cushing's syndrome: a nationwide longitudinal study," *Sleep Medicine*, vol. 36, pp. 44–47, 2017.

[18] R. T. Faghih, M. A. Dahleh, G. K. Adler, E. B. Klerman, and E. N. Brown, "Quantifying pituitary-adrenal dynamics and deconvolution of concurrent cortisol and adrenocorticotropic hormone data by compressed sensing," *IEEE Trans. Biomed. Eng.*, vol. 62, no. 10, pp. 2379–2388, 2015.

[19] R. T. Faghih, M. A. Dahleh, and E. N. Brown, "An optimization formulation for characterization of pulsatile cortisol secretion," *Frontiers in Neuroscience*, vol. 9, p. 228, 2015.